Dalton Transactions

ROYAL SOCIETY OF CHEMISTRY

COMMUNICATION

View Article Online
View Journal | View Issue

Cite this: *Dalton Trans.*, 2024, **53**, 8887

Received 26th March 2024,
Accepted 9th May 2024

DOI: 10.1039/d4dt00891j

rsc.li/dalton

A ratiometric substrate for rapid evaluation of transfer hydrogenation efficiency in solution†

Yen-An Young, Huong T. H. Nguyen, Hieu D. Nguyen, Tuhin Ganguly, Yennie H. Nguyen and Loi H. Do *

A cyclometalated iridium(III) complex bearing a self-immolative quinolinium moiety was developed as a ratiometric substrate for transfer hydrogenation studies. This photoluminescent probe allowed the rapid screening of a variety of Ir catalysts using a microplate reader, offering a convenient method to assess activity using a minimum amount of catalyst sample.

Transition metal catalysts capable of promoting transfer hydrogenation (TH), which are reactions involving the exchange of H^- equivalents between hydride donors and acceptors, have numerous applications.[1–3] For example, they are used in the stereoselective reduction of C=O and C=N groups in chemical synthesis[4,5] and the conversion of dioxygen to hydrogen peroxide in small-molecule activation[6] (Scheme 1A). Researchers have shown that TH catalysts can also be applied in living systems, including as redox modulators for anticancer therapy,[7,8] activity-based platforms for sensing endogenous formate,[9] detoxification agents against harmful aldehydes,[10] and cofactors in artificial metalloenzymes.[11,12] Although intracellular catalysts[13–15] are commonly derivatized with various ligand substituents or targeting groups,[11,16,17] such modifications risk negatively impacting their catalytic performance. Thus, having a fast and reliable method to evaluate TH catalysts could accelerate their discovery and development.

Herein, we introduce a user-friendly photoluminescence-based method to screen for TH catalyst activity using a microplate reader. Our strategy relies on the use of a ratiometric substrate that allows *in situ* quantification of the reaction progress.[18,19] This approach enables simultaneous monitoring of multiple reactions using minimum amounts of sample, which is particularly attractive for studies of catalysts that are costly (*e.g.*, those containing Ir,[20] Ru,[21] or Os[22]) or difficult to obtain on large scales.

The design of our ratiometric probe was inspired by a self-immolative umbelliferone-quinolinium substrate (**UmQN**) developed by Ward and coworkers (Scheme 1B).[11,12] It was shown that when this compound was reduced *via* TH catalysis, release of umbelliferone (**Um**) led to an emission turn-on. Although this off–on substrate was used to evaluate TH reactions in the periplasm of *E. coli*, the total amount of starting substrates inside the cells could not be quantified by fluorescence microscopy because they are non-emissive. To further complicate matters, small molecules such as substrates and molecular catalysts can diffuse in and out of cells so obtaining accurate yields in living systems is highly challenging. To overcome these limitations, we sought to develop a fluorophore-quinolinium construct that would exhibit different emission properties in the starting and product forms so that the reaction yields could be determined by monitoring the emission

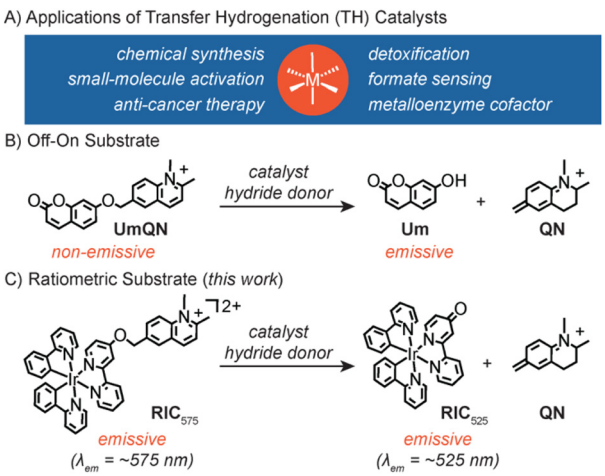

Scheme 1 Various applications of transfer hydrogenation (TH) catalysts (A) and off–on (B) and ratiometric (C) substrates used to study their activity.

Department of Chemistry, University of Houston, 4800 Calhoun Road, Houston, TX 77204, USA. E-mail: loido@uh.edu

†Electronic supplementary information (ESI) available: Experimental details, characterization data, photophysical studies, and reaction data. CCDC 2336124 and 2336125. For ESI and crystallographic data in CIF or other electronic format see DOI: https://doi.org/10.1039/d4dt00891j

intensity ratio at two different wavelengths. Such ratiometric substrates may allow non-invasive studies of intracellular TH reactions in real time without having to lyse the cells and analyse their contents by methods such as high performance liquid chromatography. After considering a variety of fluorophore candidates, we selected to use a cyclometalated iridium(III) complex as the reporter due to its tunable emission, chemical stability, and ease of preparation (Scheme 1C).[23–28] In addition, its phosphorescence may be more easily distinguished from biological self-fluorescence.[29]

The synthesis of our ratiometric iridium complex (**RIC**$_{575}$, where the subscript denotes its emission maximum) proceeded starting from 2,6-dimethylquinoline (Scheme S1†). Monobromination using *N*-bromosuccinimide (NBS) afforded compound **1** (68% yield), which was then subjected to nucleophilic attack by 2-bromo-4-hydroxypyridine to furnish **2** in 73% yield. Combining **2** in the presence of 2-(tributylstannyl)pyridine under Stille cross-coupling conditions gave the bipyridine species **3** (62% yield). Metalation of **3** was accomplished by treatment with $[Ir(ppy)_2Cl]_2$ (ppy = 2-phenylpyridine), anion exchange using AgOTf (OTf^- = triflate anion), and then alkylation using methyl triflate to afford **RIC**$_{575}$ in 38% yield (based on **3**, Scheme 2A).

The cleaved cyclometalated iridium species **RIC**$_{525}$ (where the subscript denotes its emission maximum) was also prepared (Scheme S2†). The starting 2-bromo-4-hydroxypyridine was protected using 2-methoxyethoxymethyl (MEM) chloride to give **5**, followed by Stille cross-coupling with 2-(tributylstannyl)pyridine to furnish bipyridine **6**. Combining **6** with $[Ir(ppy)_2Cl]_2$ and then treatment with HCl gave the corresponding anionic iridium complex (**RIC**$_{525'}$). To obtain the neutral form, it was stirred in the presence of NaOH, followed by the addition of AgOTf to afford **RIC**$_{525}$ with a yield of 79% based on the amount of $[Ir(ppy)_2Cl]_2$ used in the previous step.

To obtain structural characterization, X-ray crystallography was used to analyse single crystals of **RIC**$_{575}$ and **RIC**$_{525}$. The structure of **RIC**$_{575}$ showed the expected octahedral iridium center with a quinolinium moiety attached to the bipyridine ligand (Fig. S62†). The presence of two triflate anions supports the dicationic nature of the complex. The structure of **RIC**$_{525}$ also reveals an octahedral Ir geometry but the absence of any counterions in the crystallographic unit cell indicates that this species is charge neutral overall (Fig. S63†). Comparison of the bond metrics in **RIC**$_{575}$ *vs.* **RIC**$_{525}$ suggests that the former contains a 4-alkoxypyridyl donor whereas the latter contains a 4-pyridonate donor coordinated to iridium (Fig. 1A).[30–32] For example, in **RIC**$_{575}$, the C–C and C–N bond distances of ~1.33–1.39 Å in the functionalised pyridine ring are typical of an aromatic structure (Fig. 1A).[33] Additionally, its C(3)–O(1) bond length of 1.35 Å is expected for a carbon–oxygen single bond (average = ~1.37 Å). In contrast, the corresponding six-membered ring in **RIC**$_{525}$ exhibits contracted or elongated C–C/C–N bonds relative to those in **RIC**$_{575}$, suggesting that it is non-aromatic. The only exception is that the C(4)–C(5) bond distance in **RIC**$_{525}$ is similar to that in **RIC**$_{575}$ (~1.37 Å), which may be due to the conjugation of its C4 and C5 p-orbitals with the π-system of the adjacent pyridine ring. Lastly, the C(3)–O(1) bond distance of 1.28 Å in **RIC**$_{525}$ is consistent with a C=O carbonyl group.[33]

Due to the electronic differences in their ancillary ligands, **RIC**$_{575}$ and **RIC**$_{525}$ were expected to display different photophysical properties.[23] As shown in Fig. 1B, when **RIC**$_{575}$ was excited with 350 nm light in MeOH under N_2, a broad emission peak was observed with a maximum at 575 nm and shoulders at 490 and 520 nm. Our data indicate that the non-radiative decay rate (k_{nr}) was about 160-fold faster than the

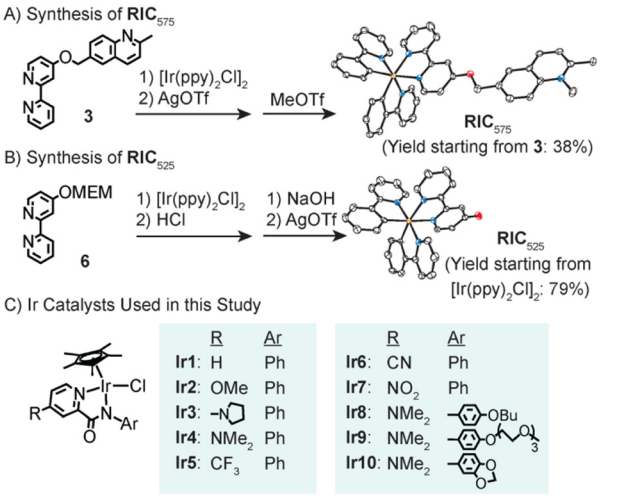

Scheme 2 Synthesis of **RIC**$_{575}$ (A) and **RIC**$_{525}$ (B) starting from their corresponding bipyridine ligands. The molecular structures of **RIC**$_{575}$ and **RIC**$_{525}$ are depicted with 50% thermal ellipsoids based on their respective X-ray crystallographic data (orange = iridium, blue = nitrogen, red = oxygen atoms). The two OTf^- anions in **RIC**$_{575}$ were omitted for clarity. In part C, the Ir catalysts used for TH studies are shown.

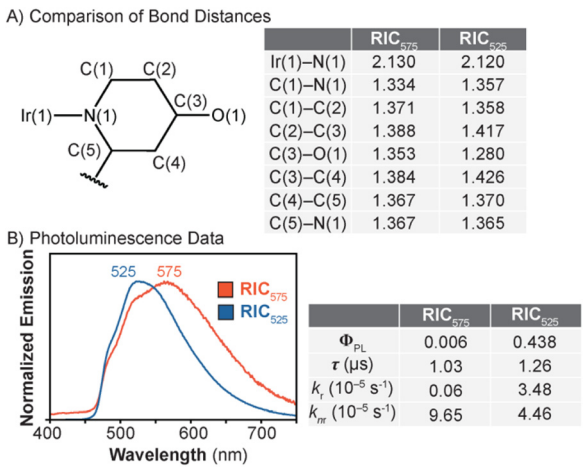

	RIC$_{575}$	RIC$_{525}$
Ir(1)–N(1)	2.130	2.120
C(1)–N(1)	1.334	1.357
C(1)–C(2)	1.371	1.358
C(2)–C(3)	1.388	1.417
C(3)–O(1)	1.353	1.280
C(3)–C(4)	1.384	1.426
C(4)–C(5)	1.367	1.370
C(5)–N(1)	1.367	1.365

	RIC$_{575}$	RIC$_{525}$
Φ_{PL}	0.006	0.438
τ (μs)	1.03	1.26
k_r (10^{-5} s^{-1})	0.06	3.48
k_{nr} (10^{-5} s^{-1})	9.65	4.46

Fig. 1 Comparison of key bond distances (Å) between **RIC**$_{575}$ and **RIC**$_{525}$ (A) and their corresponding photophysical properties (B). The emission spectra were recorded in anhydrous MeOH at 20 °C under N_2 with excitation at 350 nm.

radiative decay rate (k_r), presumably due to the emission quenching effects of its quinolinium moiety.[34] For comparison, the iridium precursor **4** bearing an unmethylated quinoline ring exhibited a k_{nr} that is only 1.9-fold faster than k_r (Table S4†). When **RIC**$_{525}$ was irradiated with 350 nm light, its emission spectrum showed a peak maximum at 525 nm. This hypsochromic shift, relative to the λ_{em} of **RIC**$_{575}$, is consistent with the more electron-rich nature of the **RIC**$_{525}$ bipyridine ligand, which destabilizes the LUMO energy and consequently, increases the Ir complex's HOMO–LUMO gap. Our results also indicate that **RIC**$_{525}$ has a higher quantum yield (Φ_{PL} = 0.438 *vs.* 0.006) and longer luminescence lifetime (τ = 1.26 *vs.* 1.03 μs) than that of **RIC**$_{575}$ (Fig. 1B). A chromaticity analysis shows that the photoluminescence of **RIC**$_{575}$ appears yellow whereas that of **RIC**$_{525}$ appears green (Fig. S4†). Because **RIC**$_{575}$ and **RIC**$_{525}$ have poor solubility in water, we were unable to perform photophysical measurements in aqueous solutions such as biological buffers or cell culture media.

Prior to conducting reaction studies with **RIC**$_{575}$, we created a calibration curve using standard solutions containing different ratios of **RIC**$_{575}$/**RIC**$_{525}$ (Table S6†). Sodium bicarbonate was also added to the mixtures to ensure that **RIC**$_{525}$ remains in the neutral form. We found that measuring the emission intensities at 550 (I_{550}) and 600 (I_{600}) nm and plotting the I_{550}/I_{600} ratio gave a linear correlation with the amount of **RIC**$_{525}$ present (Fig. S6†).[19] Due to the greater than 70-fold difference in quantum yield between **RIC**$_{525}$ and **RIC**$_{575}$, the choice of 550 and 600 nm for reaction monitoring (rather than at their emission maxima of 525 and 575 nm, respectively) ensures that signals from the product do not overwhelm signals from the starting material for accurate quantification.

Next, we proceeded to study the TH activity of a series of previously reported [Cp*Ir(4-R-picolinamidate)Cl] complexes (where Cp* = pentamethylcyclopentadienyl anion, R = various functional groups; Scheme 2C).[11,35–37] To establish that **RIC**$_{575}$ is a viable substrate for TH,[11,12] a small-scale reaction was performed using a 1-dram vial (Fig. S61A†). When **Ir4** (R = NMe_2), **RIC**$_{575}$, HCOONa, and $NaHCO_3$ were dissolved in 1 mL of MeOH and stirred at RT, the reaction mixture showed increasing luminescence over the course of 1 h with a change in color from yellow to green (Fig. S61B†), suggesting that **RIC**$_{525}$ had formed. The presence of the **RIC**$_{525}$ product was further confirmed by emission spectroscopy and mass spectrometry. Reduction of the quinolinium moiety was supported by showing that a model substrate, 1,2,6-trimethylquinolinium triflate, was converted to 1,2,3,4-tetrahydro-1,2,6-trimethylquinoline in the presence of **Ir4**, HCOONa, and $NaHCO_3$ (Fig. S59†). These results indicate that the conversion of **RIC**$_{575}$ to **RIC**$_{525}$ by the Ir catalysts and HCOONa occurs on a timescale that is suitable for quantification using a microplate reader.

Once we identified the optimal reaction conditions for TH, we carried out our catalyst screening experiments in 24-well microplates (Fig. 2A). In these investigations, each well was charged with an Ir catalyst (2.0 μM), HCOONa (0.7 mM), and $NaHCO_3$ (1.25 mM) in MeOH at 28 °C (Fig. 2A). The mixtures were injected with **RIC**$_{575}$ (0.2 mM) and then the microplate

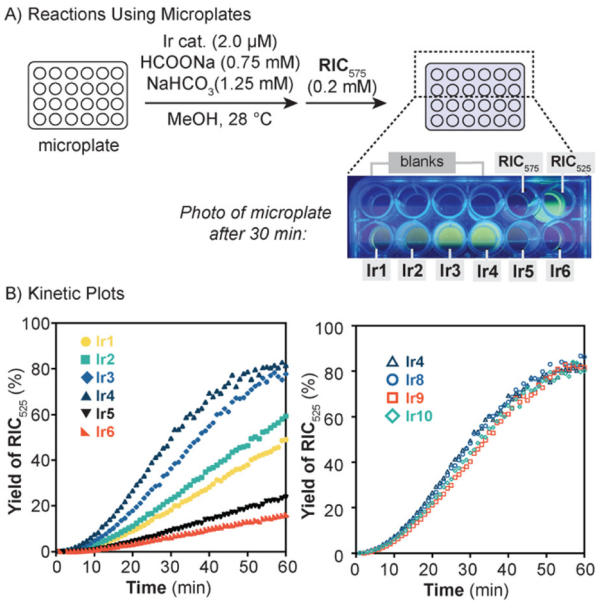

Fig. 2 (A) Scheme depicting our TH reaction studies using 24-well microplates. The photo shows a portion of the microplate after the reaction proceeded for 30 min (excitation = 325 nm light). (B) Kinetic plots of TH reactions using **RIC**$_{575}$ with catalysts **Ir1–Ir6** (left) and **Ir4/Ir8–Ir10** (right) acquired using a microplate reader.

was inserted into a microplate reader for continuous emission monitoring at 550 and 600 nm. By converting the I_{550}/I_{600} ratio to the %yield of **RIC**$_{525}$ (see Table S7† for example with **Ir1**), kinetic plots of the reactions were generated (Fig. 2B, left). The kinetic data showed that in all cases, an induction period of ~10 min was observed, which may be due to catalyst activation (*e.g.*, formation of the initial iridium-hydride species).[36] Based on the **RIC**$_{525}$ yields after 1 h, the catalyst activity trend follows the order: **Ir4** (R = NMe_2) > **Ir3** (R = pyrrolidinyl) > **Ir2** (R = OMe) > **Ir1** (R = H) > **Ir5** (R = CF_3) > **Ir6** (R = CN). The poor solubility of **Ir7**, which bears a nitro group on the pyridyl ring, precluded studies using this complex. The trend observed that electron-rich Ir catalysts are more active than their electron-poor counterparts is fully consistent with previous studies performed in aqueous media.[35,36] It has been demonstrated that hydride formation is typically rate-limiting in TH reactions by [Cp*Ir(4-R-picolinamidate)Cl] catalysts and that this step occurs faster with electron-rich than electron-poor catalysts.[36] Although a more in-depth analysis of the kinetic data was not pursued in this work, these results validate our ratiometric substrate-based approach for rapid screening of TH catalysts. Because each reaction in our studies requires only 20 nmol (<~90 μg) of Ir catalyst, a significant amount of material could be saved compared to performing larger scale reactions in standard vials or flasks.

To illustrate the utility of our method, we used our protocol to evaluate the performance of several new TH catalysts. When developing a catalyst for in cell or *in vivo* applications, it is often desirable to customize its biological properties, such as cellular uptake, interactions with biomolecules, subcellular localization, *etc.*, without diminishing its catalytic activity.[13] Because **Ir4** was

the most active in our series (Fig. 2B, left), we chose to derivatize this complex to determine whether the catalyst structure and activity could be tuned independently of each other. By adapting previously reported procedures (see ESI†), we successfully prepared three iridium variants featuring *tert*-butoxyphenyl (**Ir8**), triethylene glycol phenyl (**Ir9**), and 1,3-benzodioxole (**Ir10**) groups on the picolinamidate ligand (Scheme 2C). These substituents were chosen to represent groups with varying shapes and sizes. The new Ir catalysts were tested in TH reactions by combining them with HCOONa, $NaHCO_3$, $\mathbf{RIC}_{575}$, and MeOH in 24-well microplates. Analysis of the photoluminescence data acquired by the microplate reader produced the kinetic traces shown in Fig. 2B (right). The results revealed that **Ir8–Ir10** exhibit nearly identical kinetic profiles as that of their parent catalyst **Ir4**. This finding corroborates our previous observations that for [Cp*Ir(4-R-picolinamidate)Cl] complexes ligand modifications at the *N*-phenyl moiety do not impact their catalyst activity.[36]

In summary, we have developed a self-immolative substrate for photoluminescence monitoring of TH catalysts using a microplate reader. Because the emission maximum of the cleaved product $\mathbf{RIC}_{525}$ is blue-shifted relative to that of the starting $\mathbf{RIC}_{575}$, ratiometric quantification of the reaction yields was possible by measuring the intensity changes at two different wavelengths. Application of our method to studies of several new [Cp*Ir(4-R-picolinamidate)Cl] variants revealed that functionalization of the *N*-phenyl group does not negatively impact their catalytic activity. Our photoluminescence-based method is user-friendly because it is rapid, requires minimal catalyst sample, and can be readily used by researchers with access to microplate readers, which are available in many synthetic and biochemistry laboratories.

There are numerous non-aqueous applications that may benefit from this new molecular tool, such as in high throughput automation for chemical synthesis or metallodrug discovery.[38,39] To enable TH reaction imaging in biological cells,[40] the $\mathbf{RIC}_{575}$ probe could be rendered more water soluble by functionalizing it with sulfonate groups; however, how this change may affect its cell permeability remains to be investigated.[41] Since different cellular compartments have different pH values, modifying the probe so that its emission properties are not sensitive to pH changes could broaden its biological range. Although in-cell applications were not achieved in this work, it provides proof-of-concept demonstration that cyclometalated Ir-quinolinium substrates are useful for ratiometric quantification of TH reactions in solution.

Conflicts of interest

There are no conflicts to declare.

Acknowledgements

The authors thank the Welch Foundation (grant no. E-1894 to L. H. D.) and the National Institutes of Health (grant no. R01GM129276 to L. H. D.) for funding this work. We are grateful to Prof. Tom Teets for helpful suggestions and allowing us to use their fluorimeter.

References

1 D. Wang and D. Astruc, The Golden Age of Transfer Hydrogenation, *Chem. Rev.*, 2015, **115**, 6621–6686.
2 S. Gaillard and J.-L. Renaud, Iron-Catalyzed Hydrogenation, Hydride Transfer, and, Hydrosilylation: An Alternative to Precious-Metal Complexes?, *ChemSusChem*, 2008, **1**, 505–509.
3 A. Matsunami and Y. Kayaki, Upgrading and Expanding the Scope of Homogeneous Transfer Hydrogenation, *Tetrahedron Lett.*, 2018, **59**, 504–513.
4 P. D. Parker, X. Hou and V. M. Dong, Reducing Challenges in Organic Synthesis with Stereoselective Hydrogenation and Tandem Catalysis, *J. Am. Chem. Soc.*, 2021, **143**, 6724–6745.
5 S. Gladiali and E. Alberico, Asymmetric transfer hydrogenation: chiral ligands and applications, *Chem. Soc. Rev.*, 2006, **35**, 226–236.
6 Z. M. Heiden and T. B. Rauchfuss, Homogeneous Catalytic Reduction of Dioxygen Using Transfer Hydrogenation Catalysts, *J. Am. Chem. Soc.*, 2007, **129**, 14303–14310.
7 J. J. Soldevila-Barreda, I. Romero-Canelón, A. Habtemariam and P. J. Sadler, Transfer Hydrogenation Catalysis in Cells as a New Approach to Anticancer Drug Design, *Nat. Commun.*, 2015, **6**, 6582.
8 A. C. Carrasco, V. Rodríguez-Fanjul, A. Habtemariam and A. M. Pizarro, Structurally Strained Half-Sandwich Iridium (III) Complexes As Highly Potent Anticancer Agents, *J. Med. Chem.*, 2020, **63**, 4005–4021.
9 S. W. M. Crossley, L. Tenney, V. N. Pham, X. Xie, M. W. Zhao and C. J. Chang, A Transfer Hydrogenation Approach to Activity-Based Sensing of Formate in Living Cells, *J. Am. Chem. Soc.*, 2024, **146**, 8865–8876.
10 R. D. Jana, A. H. Ngo, S. Bose and L. H. Do, Organoiridium Complexes Enhance Cellular Defense Against Reactive Aldehydes Species, *Chem. – Eur. J.*, 2023, **29**, e202300842.
11 J. G. Rebelein, Y. Cotelle, B. Garabedian and T. R. Ward, Chemical Optimization of Whole-Cell Transfer Hydrogenation Using Carbonic Anhydrase as Host Protein, *ACS Catal.*, 2019, **9**, 4173–4178.
12 J. Zhao, J. G. Rebelein, H. Mallin, C. Trindler, M. M. Pellizzoni and T. R. Ward, Genetic Engineering of an Artificial Metalloenzyme for Transfer Hydrogenation of a Self-Immolative Substrate in *Escherichia coli's* Periplasm, *J. Am. Chem. Soc.*, 2018, **140**, 13171–13175.
13 A. H. Ngo, S. Bose and L. H. Do, Intracellular Chemistry: Integrating Molecular Inorganic Catalysts with Living Systems, *Chem. – Eur. J.*, 2018, **24**, 10584–10594.
14 H. Madec, F. Figueiredo, K. Cariou, S. Roland, M. Sollogoub and G. Gasser, Metal complexes for catalytic

and photocatalytic reactions in living cells and organisms, *Chem. Sci.*, 2023, **14**, 409–442.
15 J. J. Soldevila-Barreda and N. Metzler-Nolte, Intracellular Catalysis with Selected Metal Complexes and Metallic Nanoparticles: Advances toward the Development of Catalytic Metallodrugs, *Chem. Rev.*, 2019, **119**, 829–869.
16 M. Tomás-Gamasa, M. Martínez-Calvo, J. R. Couceiro and J. L. Mascareñas, Transition Metal Catalysis in the Mitochondria of Living Cells, *Nat. Commun.*, 2016, **7**, 12538.
17 J. W. Southwell, R. Herman, D. J. Raines, J. E. Clarke, I. Böswald, T. Dreher, S. M. Gutenthaler, N. Schubert, J. Seefeldt, N. Metzler-Nolte, G. H. Thomas, K. S. Wilson and A.-K. Duhme-Klair, Siderophore-Linked Ruthenium Catalysts for Targeted Allyl Ester Prodrug Activation within Bacterial Cells, *Chem. – Eur. J.*, 2023, **29**, e202202536.
18 M. H. Lee, J. S. Kim and J. L. Sessler, Small molecule-based ratiometric fluorescence probes for cations, anions, and biomolecules, *Chem. Soc. Rev.*, 2015, **44**, 4185–4191.
19 Z. Song, R. T. K. Kwok, E. Zhao, Z. He, Y. Hong, J. W. Y. Lam, B. Liu and B. Z. Tang, A Ratiometric Fluorescent Probe Based on ESIPT and AIE Processes for Alkaline Phosphatase Activity Assay and Visualization in Living Cells, *ACS Appl. Mater. Interfaces*, 2014, **6**, 17245–17254.
20 Y. Wei, Y. Liang, R. Luo and L. Ouyang, Recent advances of Cp*Ir complexes for transfer hydrogenation: focus on formic acid/formate as hydrogen donors, *Org. Biomol. Chem.*, 2023, **21**, 7484–7497.
21 R. Noyori and S. Hashiguchi, Asymmetric Transfer Hydrogenation Catalyzed by Chiral Ruthenium Complexes, *Acc. Chem. Res.*, 1997, **30**, 97–102.
22 J. P. C. Coverdale, C. Sanchez-Cano, G. J. Clarkson, R. Soni, M. Wills and P. J. Sadler, Easy To Synthesize, Robust Organo-osmium Asymmetric Transfer Hydrogenation Catalysts, *Chem. – Eur. J.*, 2015, **21**, 8043–8046.
23 M. S. Lowry and S. Bernhard, Synthetically Tailored Excited States: Phosphorescent, Cyclometalated Iridium(III) Complexes and Their Applications, *Chem. – Eur. J.*, 2006, **12**, 7970–7977.
24 D. N. Chirdon, C. E. McCusker, F. N. Castellano and S. Bernhard, Tracking of Tuning Effects in Bis-Cyclometalated Iridium Complexes: A Combined Time Resolved Infrared Spectroscopy, Electrochemical, and Computational Study, *Inorg. Chem.*, 2013, **52**, 8795–8804.
25 V. Mdluli, S. Diluzio, J. Lewis, J. F. Kowalewski, T. U. Connell, D. Yaron, T. Kowalewski and S. Bernhard, High-throughput Synthesis and Screening of Iridium(III) Photocatalysts for the Fast and Chemoselective Dehalogenation of Aryl Bromides, *ACS Catal.*, 2020, **10**, 6977–6987.
26 S. DiLuzio, V. Mdluli, T. U. Connell, J. Lewis, V. VanBenschoten and S. Bernhard, High-Throughput Screening and Automated Data-Driven Analysis of the Triplet Photophysical Properties of Structurally Diverse, Heteroleptic Iridium(III) Complexes, *J. Am. Chem. Soc.*, 2021, **143**, 1179–1194.
27 Y. Wu, G. D. Sutton, M. D. S. Halamicek, X. Xing, J. Bao and T. S. Teets, Cyclometalated iridium-coumarin ratiometric oxygen sensors: improved signal resolution and tunable dynamic ranges, *Chem. Sci.*, 2022, **13**, 8804–8812.
28 P.-N. Lai, C. H. Brysacz, M. K. Alam, N. A. Ayoub, T. G. Gray, J. Bao and T. S. Teets, Highly Efficient Red-Emitting Bis-Cyclometalated Iridium Complexes, *J. Am. Chem. Soc.*, 2018, **140**, 10198–10207.
29 S. Zhao, L. Chen, Y. Yang and X. Liu, Research progress of phosphorescent probe for biological imaging, *J. Mol. Struct.*, 2022, **1269**, 133855.
30 P. Beak and F. S. Fry Jr, The Equilibrium between 2-hydroxypyridine and 2-pyridone in the gas phase, *J. Am. Chem. Soc.*, 1973, **95**, 1700–1702.
31 J. DePasquale, I. Nieto, L. E. Reuther, C. J. Herbst-Gervasoni, J. J. Paul, V. Mochalin, M. Zeller, C. M. Thomas, A. W. Addison and E. T. Papish, Iridium Dihydroxybipyridine Complexes Show That Ligand Deprotonation Dramatically Speeds Rates of Catalytic Water Oxidation, *Inorg. Chem.*, 2013, **52**, 9175–9183.
32 O. E. Oladipupo, M. C. Prescott, E. R. Blevins, J. L. Gray, C. G. Cameron, F. Qu, N. A. Ward, A. L. Pierce, E. R. Collinson, J. F. Hall, S. Park, Y. Kim, S. A. McFarland, I. Fedin and E. T. Papish, Ruthenium Complexes with Protic Ligands: Influence of the Position of OH Groups and π Expansion on Luminescence and Photocytotoxicity, *Int. J. Mater. Sci.*, 2023, **24**, 5980.
33 A. G. Orpen, L. Brammer, F. H. Allen, O. Kennard, D. G. Watson and R. Taylor, Appendix A: Typical Interatomic Distances in Organic Compounds and Organometallic Compounds and Coordination Complexes of the d- and f-block metals, *Structure Correlation*, 1994, 751–858.
34 K. L. VanDenburgh, Y. Liu, T. Sadhukhan, C. R. Benson, N. M. Cox, S. Erbas-Cakmak, B. Qiao, X. Gao, M. Pink, K. Raghavachari and A. H. Flood, Multi-state amine sensing by electron transfers in a BODIPY probe, *Org. Biomol. Chem.*, 2020, **18**, 431–440.
35 A. H. Ngo, M. Ibañez and L. H. Do, Catalytic Hydrogenation of Cytotoxic Aldehydes Using Nicotinamide Adenine Dinucleotide (NADH) in Cell Growth Media, *ACS Catal.*, 2016, **6**, 2637–2641.
36 A. H. Ngo and L. H. Do, Structure–Activity Relationship Study of Half-Sandwich Metal Complexes in Aqueous Transfer Hydrogenation Catalysis, *Inorg. Chem. Front.*, 2020, **7**, 583–591.
37 Z. Almodares, S. J. Lucas, B. D. Crossley, A. M. Basri, C. M. Pask, A. J. Hebden, R. M. Phillips and P. C. McGowan, Rhodium, Iridium, and Ruthenium Half-Sandwich Picolinamide Complexes as Anticancer Agents, *Inorg. Chem.*, 2014, **53**, 727–736.
38 C. W. Coley, N. S. Eyke and K. F. Jensen, Autonomous Discovery in the Chemical Sciences Part I: Progress, *Angew. Chem., Int. Ed.*, 2020, **59**, 22858–22893.
39 C. W. Coley, N. S. Eyke and K. F. Jensen, Autonomous Discovery in the Chemical Sciences Part II: Outlook, *Angew. Chem., Int. Ed.*, 2020, **59**, 23414–23436.

40 J. Cui, S. Zang, H. Nie, T. Shen, S. Su, J. Jing and X. Zhang, An ICT-based fluorescent probe for ratiometric monitoring the fluctuations of peroxynitrite in mitochondria, *Sens. Actuators, B*, 2021, **328**, 129069.

41 M. R. Schreier, X. Guo, B. Pfund, Y. Okamoto, T. R. Ward, C. Kerzig and O. S. Wenger, Water-Soluble Tris(cyclometalated) Iridium(III) Complexes for Aqueous Electron and Energy Transfer Photochemistry, *Acc. Chem. Res.*, 2022, **55**, 1290–1300.